Ti=NR vs Ti−R′ Functional Group Selectivity in Titanium Imido Alkyl Cations from a DFT Perspective

Marta Feliz,[†] Paul D. Bolton,[‡] Philip Mountford,*[,‡] and Eric Clot*[,†]

Institut Charles Gerhardt Montpellier, UMR 5253 CNRS-UM2-ENSCM-UM1, cc 1501, Place Eugène Bataillon, F-34095 Montpellier Cedex 5, France, and Chemistry Research Laboratory, University of Oxford, Mansfield Road, Oxford OX1 3TA, U.K.

Received July 26, 2008

The reactions of Ti(N^{t}Bu)(Me$_3$[9]aneN$_3$)Me$^+$ (**1**) with a series of polar and nonpolar unsaturated organic substrates give different kinds of products, resulting either from cycloaddition to the Ti=N bond (PhCCH) or from insertion into the Ti−Me bond (PhCCPh, ^{i}PrNCN^{i}Pr, ethylene polymerization). DFT(B3PW91) calculations of the reaction pathways for cycloaddition and insertion on small model systems illustrate the basic electronic properties in terms of reaction site selectivity. In all cases the cycloaddition is shown to be the preferred pathway kinetically. ONIOM(B3PW91:HF) calculations on the experimental systems allow the evaluation of the influence of the steric bulk of the ligand set on the outcome of the reaction. Introduction of the actual ligands results essentially in a destabilization of the cycloaddition pathway and leads both to a cancellation of the kinetic preference for cycloaddition and to a reduced thermodynamic stability of the cycloaddition product. Only for the terminal alkyne PhCCH does cycloaddition remain the preferred pathway. For all the other substrates, insertion and cycloaddition are kinetically competitive, but insertion is thermodynamically much favored. In the case of Ti(N^{t}Bu)(Me$_3$[9]aneN$_3$)Cl$^+$ (**2**), where insertion is not possible, the calculations show that cycloaddition is endothermic with respect to coordination, explaining the experimental results (coordination for ^{i}PrNCN^{i}Pr and absence of reaction for PhCCPh and C_2H_4). Only in the case of PhCCH is cycloaddition favored with **2**. ONIOM calculations on a Zr analogue of **1** show that, for the larger metal, the steric bulk does not destabilize the cycloaddition pathway enough to make insertion competitive.

Introduction

d^0 transition-metal imido complexes are active species in many different catalytic processes. One prominent example is the Schrock olefin metathesis catalyst family M(NR)(CHR′)(OR″)$_2$ (M = Mo, W), widely exploited in organic and inorganic applications[1] and comprehensively studied computationally.[2] In these complexes the imido ligand plays a "supporting" or "spectator" role and the $2\pi + 2\pi$ cycloaddition reaction site selectivity of ethylene for the Mo=CH$_2$ bond was explained by Ziegler in terms of both kinetic and thermodynamic preferences.[2e] However, the imido ligand can play an active (nonspectator) role, as in the catalytic cycle for hydroamination of alkynes and allenes.[3] Here the key step is a $2\pi + 2\pi$ cycloaddition of the alkyne with the M=NR bond to generate an azametallacyclobutene complex. The calculations by Straub and Bergman on CpTi(NH)(NH$_2$) have shown that cycloaddition is a very easy process with an activation barrier lower than 1 kJ mol^{-1} and exothermic formation of a very stable azatitanacyclobutene ($\Delta G = -82.4$ kJ mol^{-1}).[4] This is in agreement with the observation that coupling reactions of the M=NR functional group (especially for group 4 metals) with unsaturated organic and other substrates are found to be facile.[5]

Imido supporting ligands have also been exploited in the development of post-metallocene Ziegler-type olefin polymerization catalysts,[6] another highly topical area of transition-metal research.[7] The active species in early-transition-metal Ziegler catalysts are alkyl cations [(L)MR]$^+$ (L = supporting ligand or

* To whom correspondence should be addressed. E-mail: philip.mountford@chem.ox.ac.uk (P.M.); clot@univ-montp2.fr (E.C.).
† Institut Charles Gerhardt.
‡ University of Oxford.

(1) (a) Schrock, R. R. *Acc. Chem. Res.* **1990**, *23*, 158. (b) Schrock, R. R. *Pure Appl. Chem.* **1994**, *66*, 1447. (c) Schrock, R. R. *Dalton Trans.* **2001**, 2541. (d) Schrock, R. R.; Hoveyda, A. H. *Angew. Chem., Int. Ed.* **2003**, *42*, 4592. (e) Schrock, R. R. *Angew. Chem., Int. Ed.* **2006**, *45*, 3748. (f) Chauvin, Y. *Angew. Chem., Int. Ed.* **2006**, *45*, 3740.

(2) (a) Rappé, A. K.; Goddard, W. A., III *J. Am. Chem. Soc.* **1982**, *104*, 448. (b) Sodupe, M.; Lluch, J. M.; Oliva, A.; Bertran, J. *New J. Chem.* **1991**, *15*, 321. (c) Folga, E.; Ziegler, T. *Organometallics* **1993**, *12*, 325. (d) Wu, Y.-D.; Peng, Z.-H. *J. Am. Chem. Soc.* **1997**, *119*, 8043. (e) Monteyne, K.; Ziegler, T. *Organometallics* **1998**, *17*, 5901. (f) Wu, Y.-D; Peng, Z.-H. *Inorg. Chim. Acta* **2003**, *345*, 241. (g) Goumans, T. P. M.; Ehlers, A. W. *Organometallics* **2005**, *24*, 3200. (h) Poater, A.; Solans-Monfort, X.; Clot, E.; Copéret, C.; Eisenstein, O. *J. Am. Chem. Soc.* **2007**, *129*, 8207.

(3) (a) Pohlki, F.; Doyle, S. *Chem. Soc. Rev.* **2003**, *32*, 104. (b) Bytschkov, I.; Doye, S. *Eur. J. Inorg. Chem.* **2003**, 935. (c) Tillack, A.; Jiao, H.; Castro, I. G.; Hartung, C. G.; Beller, M. *Chem. Eur. J.* **2004**, *10*, 2409. (d) Tillack, A.; Khedkar, V.; Jiao, H.; Beller, M. *Eur. J. Inorg. Chem.* **2005**, 5001. (e) Odom, A. L. *Dalton Trans.* **2005**, 225.

(4) Straub, B. F.; Bergman, R. G. *Angew. Chem., Int. Ed.* **2001**, *40*, 4632.

(5) (a) Wigley, D. E. *Prog. Inorg. Chem.* **1994**, *42*, 239. (b) Mountford, P. *Chem. Commun.* **1997**, 2127. (c) Gade, L. H.; Mountford, P. *Coord. Chem. Rev.* **2001**, *216−217*, 65. (d) Duncan, A. P.; Bergman, R. G. *Chem. Rec.* **2002**, *2*, 431. (e) Hazari, N.; Mountford, P. *Acc. Chem. Res.* **2005**, *38*, 839.

(6) Bolton, P. D.; Mountford, P. *Adv. Synth. Catal.* **2005**, *347*, 355.

(7) (a) Brintzinger, H. H.; Fischer, D.; Mülhaupt, R.; Rieger, B.; Waymouth, R. M. *Angew. Chem., Int. Ed. Engl.* **1995**, *34*, 1143. (b) Bochmann, M. *J. Chem. Soc., Dalton Trans.* **1996**, 255. (c) Kaminsky, W. *J. Chem. Soc., Dalton Trans.* **1998**, 1413. (d) Resconi, L.; Cavallo, L.; Fait, A.; Piemontesi, F. *Chem. Rev.* **2000**, *100*, 1253. (e) Itell, S. D.; Johnson, L. K.; Brookhart, M. *Chem. Rev.* **2000**, *100*, 1169. (f) Gibson, V. C.; Spitzmesser, S. K. *Chem. Rev.* **2003**, *103*, 283. (g) Mitani, M.; Saito, J.; Ishii, S.; Nakayama, Y.; Makio, H.; Matsukawa, N.; Matsui, S.; Mohri, J.; Furuyama, R.; Terao, H.; Bando, H. H.; Fujita, T. *Chem. Rec.* **2004**, *4*, 137. (h) Stephan, D. W. *Organometallics* **2005**, *24*, 2548.

10.1021/om8007103 CCC: $40.75
Publication on Web 10/29/2008

Scheme 1. Reactions of Ti(N^{t}Bu)(Me$_3$[9]aneN$_3$)Me$^+$ (1, Left) and Ti(N^{t}Bu)(Me$_3$[9]aneN$_3$)Cl$^+$ (2, Right) with Unsaturated Substrates[a]

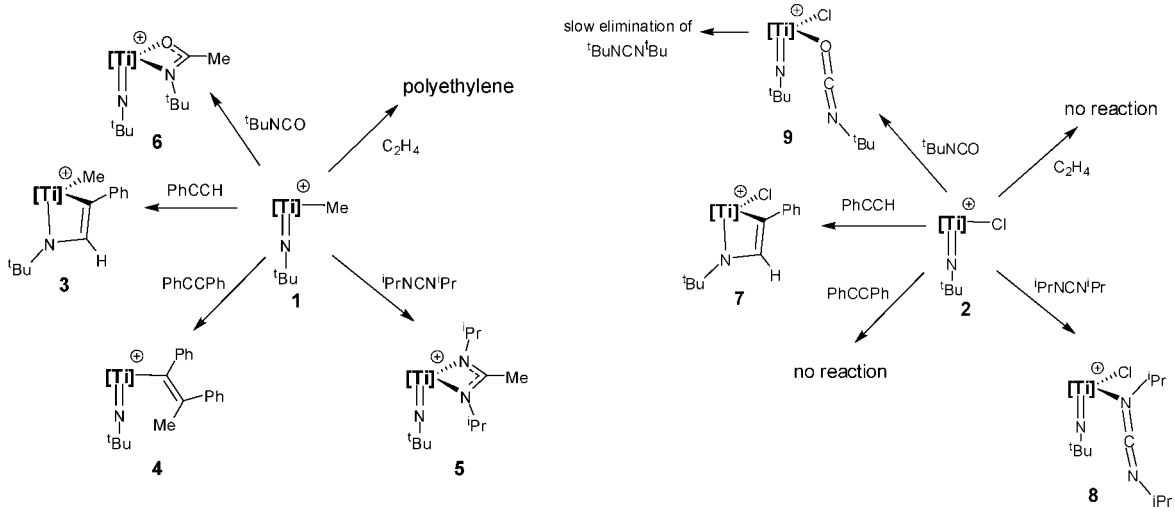

[a] **[Ti]** = Ti(Me$_3$[9]aneN$_3$).

Scheme 2. Potential Products of the Reaction of Ti(N^{t}Bu)(Me$_3$[9]aneN$_3$)Me$^+$ (1) with PhCCH

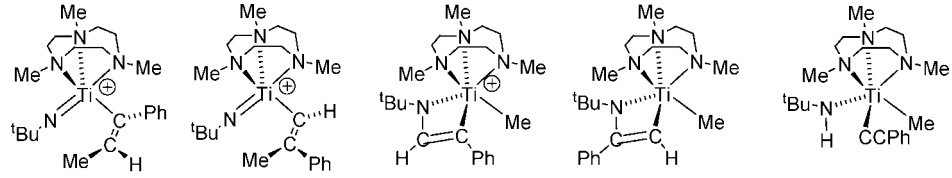

ligand set, R = initiating alkyl group or polymeryl chain).[8] Even though the chemistry of early-transition-metal alkyl cations in general is well understood, very few studies have looked at the question of reaction site selectivity in imido compounds (neutral or cationic) that also feature a metal−alkyl bond,[9] and there are no reports combining DFT and experimental studies of the well-defined systems. Of relevance in this regard is Gibson's report that the chromium bis(imido) systems Cr(NR)$_2$X$_2$ (R = alkyl, aryl; X = Cl, CH$_2$Ph) form moderately active olefin polymerization catalysts with suitable activators.[10] These researchers also described limited in situ spectroscopic evidence for the benzyl cation [Cr(N^{t}Bu)$_2$(CH$_2$Ph)]$^+$ and a PMe$_3$ adduct. Jensen and Børve reported DFT studies of the reaction of the model cation [Cr(NH)$_2$Me]$^+$ with C$_2$H$_4$ and found that, while insertion of C$_2$H$_4$ into the Cr−Me bond was thermodynamically favored, cycloaddition to Cr═NH was kinetically the more preferred route.[11] However, this prediction has not been tested experimentally.

The imido-supported Ziegler catalyst family of the type Ti(NR)(Me$_3$[9]aneN$_3$)Cl$_2$ is the most active and also most systematically studied of this class of compounds.[12−14] Structure−activity relationship studies using high-throughput screening techniques found that bulky imido N substituents "R" were prerequisites for high catalytic productivities (e.g., R = ^{t}Bu, adamantyl, CMe$_2$CH$_2$^{t}Bu), especially at the commercially relevant high operating temperatures that these catalysts tolerate.[12] In pursuit of a better understanding of the catalyst Ti(NR)(Me$_3$[9]aneN$_3$)Cl$_2$, we recently reported that the thermally stable alkyl Ti(N^{t}Bu)(Me$_3$[9]aneN$_3$)Me$_2$ is cleanly and quantitatively converted to the well-defined cation Ti(N^{t}Bu)(Me$_3$[9]aneN$_3$)Me$^+$ (**1**) by treatment with [CPh$_3$][BAr$_4^F$] (Ar^F = C$_6$F$_5$).[13] The chloride cation Ti(N^{t}Bu)(Me$_3$[9]aneN$_3$)Cl$^+$ (**2**) was also readily accessed from Ti(N^{t}Bu)(Me$_3$[9]aneN$_3$)(Me)Cl.[13b] The reactions of **1** and **2** with a series of polar and nonpolar unsaturated organic substrates were studied experimentally (Scheme 1) as described in the preceding paper.[14]

In this contribution we describe DFT(B3PW91) and ONIOM (B3PW91:HF) calculations on key representative examples of these reactions as described in Scheme 1. DFT(B3PW91) calculations on small model systems illustrate the basic electronic properties in terms of reaction site selectivity, while ONIOM(B3PW91:HF) calculations allow the evaluation of the influence of the steric bulk in the ligand set (R$_3$[9]aneN$_3$ and

(8) (a) Jordan, R. F. *Adv. Organomet. Chem.* **1991**, *32*, 325. (b) Grubbs, R. H.; Coates, G. W. *Acc. Chem. Res.* **1996**, *29*, 85. (c) Bochmann, M. *J. Chem. Soc., Dalton Trans.* **1996**, 255.

(9) (a) Ward, B. D.; Orde, G.; Clot, E.; Cowley, A. R.; Gade, L. H.; Mountford, P. *Organometallics* **2004**, *23*, 4444. (b) Ward, B. D.; Orde, G.; Clot, E.; Cowley, A. R.; Gade, L. H.; Mountford, P. *Organometallics* **2005**, *24*, 2368. (c) Anderson, L. L.; Schmidt, J. A. R.; Arnold, J.; Bergman, R. G. *Organometallics* **2006**, *25*, 3394.

(10) Coles, M. P.; Dalby, C. I.; Gibson, V. C.; Little, I. R.; Marshall, E. L.; Ribeiro da Costa, M. H.; Mastroianni, S. *J. Organomet. Chem.* **1999**, *591*, 78.

(11) (a) Jensen, V. R.; Børve, K. J. *Organometallics* **2001**, *20*, 616. (b) Jensen, V. R.; Børve, K. J. *Chem. Commun.* **2002**, 542.

(12) (a) Adams, N.; Arts, H. J.; Bolton, P. D.; Cowell, D.; Dubberley, S. R.; Friederichs, N.; Grant, C.; Kranenburg, M.; Sealey, A. J.; Wang, B.; Wilson, P. J.; Cowley, A. R.; Mountford, P.; Schröder, M. *Chem. Commun.* **2004**, 434. (b) Adams, N.; Arts, H. J.; Bolton, P. D.; Cowell, D.; Dubberley, S. R.; Friederichs, N.; Grant, C.; Kranenburg, M.; Sealey, A. J.; Wang, B.; Wilson, P. J.; Zuideveld, M. A.; Blake, A. J.; Schröder, M.; Mountford, P. *Organometallics* **2006**, *25*, 3888. (c) Bolton, P. D.; Adams, N.; Clot, E.; Cowley, A. R.; Wilson, P. J.; Schröder, M.; Mountford, P. *Organometallics* **2006**, *25*, 5549.

(13) (a) Bolton, P. D.; Clot, E.; Cowley, A. R.; Mountford, P. *Chem. Commun.* **2005**, 3313. (b) Bolton, P. D.; Clot, E.; Adams, N.; Dubberley, S. R.; Cowley, A. R.; Mountford, P. *Organometallics* **2006**, *25*, 2806.

(14) Bolton, P. D.; Feliz, M.; Cowley, A. R.; Clot, E.; Mountford, P. *Organometallics* **2008**, *27*, 6096.

Table 1. Energies (kJ mol^{-1}) of the various TS for the Reaction between 1 and PhCCH (taken as Origin of Energy)[a]

	TSInsSyn	TSInsAnti	TSCycSyn	TSCycAnti	TS12
E(B3PW91)	11.3	−10.0	−19.9	−10.9	−15.1
E(ONIOM)	11.7	−9.5	−15.6	−4.3	−17.0
E′(B3PW91)	11.3	−11.1	−19.9	−9.8	−15.6

[a] *E*(B3PW91) corresponds to B3PW91 optimizations on the real systems, *E*(ONIOM) is the extrapolated energy from geometries optimized at the ONIOM(B3PW91:HF) level, and *E′*(B3PW91) is the B3PW91 energy of the ONIOM geometry (B3PW91//ONIOM (B3PW91:HF)).

imido ligand) on the outcome of the reaction.[15] These studies bring a complementary view of the reactivity of these cations and, together with the experimental work, provide a comprehensive insight into the reaction site selectivity in polymerization-active transition-metal cations which contain both a M═NR and M−R′ functional group as potential sites for $2\pi + 2\pi$ cycloaddition or migratory insertion.

Results and Discussion

The aim of the paper is first to highlight the basic electronic preferences in reactive site selectivity and then to explore how steric bulk may alter these preferences. Reactions of **1** or **2** with PhCCH, PhCCPh, ^{i}PrNC^{i}Pr, and C_2H_4 have been chosen as representative ones and addressed computationally. Full DFT(B3PW91) calculations have been carried out on model systems where the real cations **1** and **2** have been simplified as Ti(NMe)(H$_3$[9]aneN$_3$)X$^+$ (X = Me, **1q**; X = Cl, **2q**) and the substrates are MeCCMe, MeNCNMe, and C_2H_4, respectively. Calculations on the real systems have been performed at the ONIOM(B3PW91:HF) level.

1. Terminal Alkynes: Reaction with PhCCH. Bergman and Andersen found that Cp*$_2$Ti(NPh) reacted with HCCH to give a cycloaddition product. Using RCCH (R = Ph, SiMe$_3$) gave 1,2-C−H addition to Ti═NPh.[16] Wolczanski found that transient Ti(NPh)(^{t}Bu$_3$SiO)$_2$ reacted irreversibly, with both internal and terminal alkynes forming only cycloaddition products—no 1,2-addition was observed.[17] Using a diamide−amine ligand, Gade and Mountford found that PhCCH underwent anti-Markovnikov cycloaddition to Ti═N^{t}Bu, whereas in fact MeCCMe and PhCCMe gave products of methyl C−H activation.[18] Beller et al. have studied experimentally the regiochemistry of the cycloaddition of terminal alkynes to the Ti═NR linkage.[3c,d] Hydroamination of RCCH (R = alkyl) with ^{t}BuNH$_2$ yielded exclusively the anti-Markovnikov imine, thus implying that the azatitanacyclobutene formed had the same geometry as that described for **3** (Scheme 1). Outside of group 4, Bercaw et al. observed that Cp$_2$*Ta(N^{t}Bu)(THF)$^+$ reacts with MeCCH at 25 °C to yield a mixture of Cp$_2$*Ta(HN^{t}Bu)(CCMe)$^+$ (60%) and the azatantalacyclobutene Cp$_2$*Ta{^{t}BuNC(H)CMe}$^+$ (40%).[19] Upon heating to 60 °C the latter was converted into the former, thus showing that cycloaddition is a reversible process.

Experimentally (Scheme 1), the cycloaddition product **3** (designated **ProdCycSyn** in Scheme 2) is the only one observed in the reaction of the methyl cation **1** with PhCCH. However, there are in fact potentially five different products that can be obtained upon reaction of PhCCH with **1** (Scheme 2). In order to calibrate the ONIOM calculations to be described later, DFT(B3PW91) calculations on the transition states associated with formation of each product have been searched for **1** reacting with PhCCH and are shown in Figure 1. The energy of each TS with respect to separated reactants **1** and PhCCH is given in Table 1. In agreement with the experimental observations, the lowest transition state is **TSCycSyn**, leading to the $2\pi + 2\pi$ cycloaddition product with the alkyne hydrogen toward the imido ^{t}Bu group. As expected, on the basis of steric constraint arguments, the other TS for cycloaddition, **TSCycAnti**, featuring a phenyl group close to the imido substituent, lies at higher energy. The two TS for insertion into Ti−Me are higher in energy, in particular **TSInsSyn**, where the Ph group is repelled by the equatorial Me group of the Me$_3$[9]aneN$_3$ ligand.[20] C−H activation of PhCCH is also possible through 1,2-addition to Ti═N^{t}Bu (transition state **TS12**).[16] **TS12** was computed to be at higher energy than **TSCycSyn**.

In order to have a better estimate of the relative energies of the various TS, single-point calculations on the B3PW91 geometries have been performed with 14 different functionals, even including the double-hybrid functional MPW2PLYP recently developed by Grimme (Table S1 in the Supporting Information).[21] All of the functionals reproduce the experimental selectivity, with **TSCycSyn** being the lowest TS. On average the other TS are at least 10 kJ mol^{-1} higher in energy. The basic reactive properties of **1** are faithfully reproduced with the B3PW91 functional. However, full DFT calculations on the real systems are computationally prohibitively demanding and we therefore considered ONIOM calculations.

As a test of the ONIOM method for these systems, the five transition states in Figure 1 have been optimized at the ONIOM(B3PW91:HF) level. In the ONIOM calculations, the Me groups on both the Me$_3$[9]aneN$_3$ ligand and the ^{t}Bu group, and also the Ph group on the alkyne were treated at the HF level. The ONIOM extrapolated energies *E*(ONIOM) of these TS are given in Table 1, and from these values the predicted kinetically preferred pathway is 1,2-addition to Ti═N, which is not the situation found experimentally.[14] However, the geometries obtained with ONIOM are very close to the DFT ones, as illustrated by selected geometrical parameters reported in Table S2 in the Supporting Information. Indeed, single-point B3PW91 calculations on the ONIOM geometries (B3PW91//ONIOM(B3PW91:HF), designated *E′*(B3PW91) in Table 1) yielded values very similar to those obtained with DFT. Also in this case, the pathway observed experimentally (**TSCycSyn**) is found as the kinetically preferred one, although the energy differences with **TS12** are rather small and method dependent. Nevertheless, in the remainder of the paper, for the real systems, ONIOM(B3PW91:HF) calculations will be performed and only B3PW91 single-point energy values obtained on the ONIOM geometries (B3PW91//ONIOM(B3PW91:HF)) will be discussed.

No π-alkyne complexes could be optimized as precomplexes before cycloaddition or insertion. Nonetheless, the energy values of the various TS in Table 1 are mostly negative, implying stabilization of the system prior to reaction. This is in fact accounted for by σ-coordination of the C−H bond of PhCCH.

(15) The focus of the study is on Ti═NR vs Ti−R′ site selectivity in titanium imido alkyl cations; therefore, neither anion effects nor solvent influences have been considered in the present work.

(16) Polse, J. L.; Andersen, R. A.; Bergman, R. G. *J. Am. Chem. Soc.* **1998**, *120*, 13405.

(17) Bennet, J. L.; Wolczanski, P. T. *J. Am. Chem. Soc.* **1997**, *119*, 10696.

(18) (a) Bashall, A.; McPartlin, M.; Collier, P. E.; Mountford, P.; Gade, L. H.; Trösch, D. J. M. *Chem. Commun.* **1998**, 2555. (b) Ward, B. D.; Maisse-François, A.; Mountford, P.; Gade, L. H. *Chem. Commun.* **2004**, 704.

(19) Blake, R. E., Jr.; Antonelli, D. M.; Henling, L. M.; Schaefer, W. P.; Hardcastle, K. I.; Bercaw, J. E. *Organometallics* **1998**, *17*, 718.

(20) Throughout the text "equatorial" and "axial" refer to coordination sites cis and trans to Ti═NR, respectively.

(21) Schwabe, T.; Grimme, S. *Phys. Chem. Chem. Phys.* **2006**, *8*, 4398.

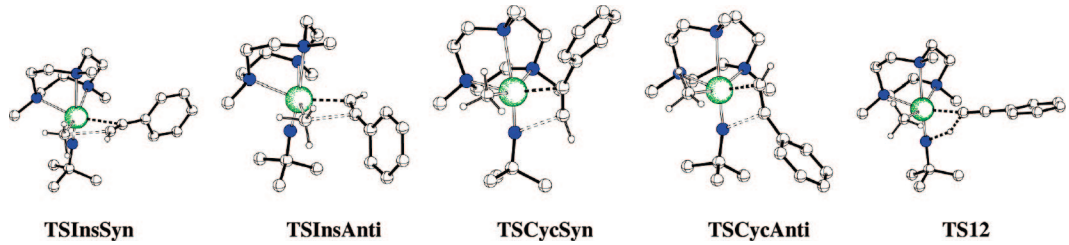

Figure 1. B3PW91 optimized geometries of the transition states for the five different reactions possible between **1** and PhCCH.

Three different σ-CH complexes of PhCCH could be located at the ONIOM(B3PW91:HF) level, and their geometries and energies are given in Figure S1 of the Supporting Information. The stability of ca. 30−40 kJ mol^{-1} of these precomplexes is not enough to compensate for the loss of entropy and explains why they are not observed experimentally. However, calculating entropy in the condensed phase is not an easy task. Various alternatives have been suggested in the literature, including even the full neglect of the translational entropy, which is the greatest contribution to the total entropy changes.[22] In the present work we are essentially interested in reactions of the type A + B → C (see Scheme 1) where the major contribution to the Gibbs free energy is loss of translational entropy. For all the processes studied in this work, the translational entropy contribution $-T\Delta S_t$ has been evaluated at $T = 298$ K and the average value is +47.3 kJ mol^{-1}. Thus changes in Gibbs free energy (ΔG) would be arbitrarily estimated by adding 50 kJ mol^{-1} to the electronic energy for the respective transition states and intermediates. This allows one to obtain a qualitative idea of the stability of a given species with respect to separated reactants. However, when the relative stabilities of two different isomers or transition states are compared, using only electronic energy values is quantitatively accurate, as entropic contributions are expected to be similar when the number of particles is conserved.

We turn now to the thermodynamic stabilities of the various products listed in Scheme 2. Figure 2 shows schematically the relative energies of the various products and transition states as obtained from ONIOM(B3PW91:HF) calculations. Only the most stable precomplex, **1-σ_1**, is shown in Figure 2, which serves as a starting point for all subsequent transformations. Even though the products of Ti−Me bond insertion are calculated to be the most thermodynamically stable molecules (−184.0 kJ mol^{-1}, **ProdInsSyn**; −169.2 kJ mol^{-1}, **ProdInsAnti**), the experimentally observed kinetic product of cycloaddition **ProdCycSyn** is nonetheless calculated to be thermodynamically stable (−156.1 kJ mol^{-1}) in an absolute sense. Furthermore, **ProdCycSyn** is substantially more stable than the product of 1,2-addition of C−H to Ti=N^{t}Bu (−88.0 kJ mol^{-1}, **Prod12**), which was kinetically a competitive pathway. Note that the computed ^{1}H NMR chemical shift for the alkyne-derived PhCC*H* hydrogen in **ProdCycSyn** (11.4 ppm) compares very well with the experimental value found for **3** (11.38 ppm), whereas the values in the 1,2-addition isomer **Prod12** (8.7 ppm) and in the insertion products **ProdInsSyn** (6.8 ppm) and **ProdInsAnti** (8.2 ppm) are significantly different, supporting the experimental structural assignment.

The corresponding product of cycloaddition of PhCCH with the chloride cation **2**, **ProdCycSynCl** (designated **7** in Scheme 1 for the experimental system), has been optimized at the ONIOM level only for the regioisomer with H adjacent to ^{t}Bu. The electronic energy of −151.0 kJ mol^{-1} is similar to that of **ProdCycSyn** for reaction of PhCCH with the methyl cation **1**, in agreement with the experimental observation of a cycloaddition product.[14] Moreover, the computed chemical shift of 11.7 ppm for the hydrogen atom in **ProdCycSynCl** compares very well with that of 11.68 ppm in **7**.

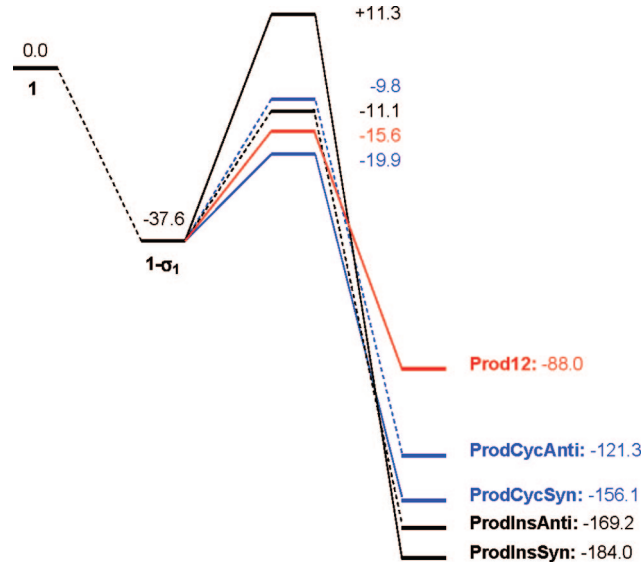

Figure 2. Schematic representation of the various pathways (cycloaddition in blue, insertion in black, and 1,2-C−H addition in red) for PhCCH reacting with **1**. B3PW91 energies (kJ mol^{-1}) on ONIOM(B3PW91:HF) geometries are given (B3PW91//ONIOM(B3PW91:HF)).

2. Internal Alkynes: Reactions with MeCCMe and PhCCPh. Experimentally (Scheme 1) reactions of **1** with PhCCPh and PhCCSiMe$_3$ gave well-defined products of Ti−Me bond insertion.[14] However, to probe the basic electronic preferences generally in the case of internal alkynes, simplified model systems were first considered. 2-Butyne was used as a model for internal alkynes, and the simplified cation Ti(NMe)(H$_3$[9]aneN$_3$)Me$^+$ (**1q**) was considered as a model for the real monomethyl cation **1**.

Coordination of MeCCMe to **1q** is exothermic ($\Delta E = -59.1$ kJ mol^{-1}) and leads to the π complex **1q-π-yne** with the C≡C bond aligned with the Ti=N bond vector (Figure 3). This is in contrast to the σ complex **1-σ_1** formed with PhCCH. The coordination of the alkyne is asymmetric, with one Ti−C bond being longer than the other (2.400 Å vs 2.529 Å). The long Ti···C bond is associated with a short N···C contact (2.732 Å) for the imido ligand. The C≡C bond is slightly elongated upon coordination (1.195 Å, 2-butyne; 1.231 Å, **1q-π-yne**). From **1q-π-yne** (see Figure 4 for an energy diagram), the 2π + 2π cycloaddition proceeds easily through **1q-TSCyc-yne** ($\Delta E^{\ddagger} = 1.6$ kJ mol^{-1}) to yield the cycloaddition product **1q-**

(22) (a) Cooper, J.; Ziegler, T. *Inorg. Chem.* **2002**, *41*, 6614. (b) Sakaki, S.; Takayama, T.; Sumimoto, M.; Sugimoto, M. *J. Am. Chem. Soc.* **2004**, *126*, 3332. (c) Rotzinger, F. P. *Chem. Rev.* **2005**, *105*, 2003. (d) Leung, B. O.; Reidl, D. L.; Armstrong, D. A.; Rauk, A. *J. Phys. Chem. A* **2004**, *108*, 2720. (e) Ardura, D.; Lopez, R.; Sordo, T. L. *J. Phys. Chem. B* **2005**, *109*, 23618.

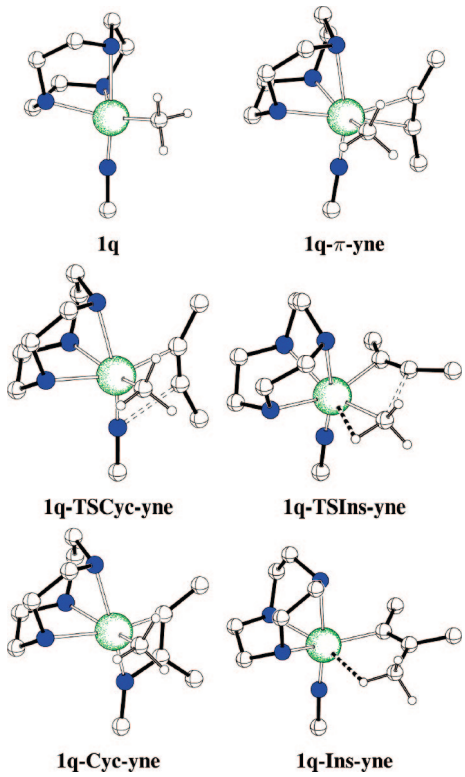

Figure 3. B3PW91 optimized geometries of the extrema located along the pathways for reaction of $Ti(H_3[9]aneN_3)(NMe)Me^+$ (**1q**) with MeCCMe: (a) cycloaddition of 2-butyne to Ti=NMe (left); (b) insertion of 2-butyne into Ti−Me (right). Only H atoms on the methyl ligand are shown for clarity.

Cyc-yne in a reasonably exothermic process ($\Delta E = -99.8$ kJ mol^{-1}). These energy values are very similar to those obtained by Straub and Bergman for $CpTi(NH_2)(NH)$ ($\Delta E^{\ddagger} = 0.5$ kJ mol^{-1} and $\Delta E = -101.2$ kJ mol^{-1}).[4] In **1q-TSCyc-yne**, the Ti−C bonds get shorter, still maintaining the asymmetry (2.204 and 2.388 Å), and the N···C contact gets shorter (2.397 Å). As a result of the cycloaddition, the Ti=N bond lengthens (1.694 Å, **1q-π-yne**; 1.712 Å, **1q-TSCyc-yne**). **1q-Cyc-yne** deserves no special comments, and the azatitanacyclobutene exhibits Ti−N bonds shorter than Ti−C bonds (1.883 vs 1.922 Å, respectively) and N−C_β bonds longer than C_α−C_β bonds (1.412 vs 1.405 Å, respectively).

No π-complex with the C≡C bond lying in the equatorial plane could be optimized as a local minimum on the PES. Therefore, **1q-π-yne** serves as a precomplex for insertion of 2-butyne into the Ti−C bond. The transition state **1q-TSIns-yne** has been located on the PES (Figure 3) and lies 50.7 kJ mol^{-1} above **1q-π-yne**. In **1q-TSIns-yne** the Ti−Me bond elongates (2.128 Å, **1q-π-yne**; 2.134 Å, **1q-TSIns-yne**) and the methyl group presents an α-CH agostic interaction (C_α−H_α = 1.121 Å, H_α···Ti = 2.132 Å, Ti−C_α−H_α = 74.6°). The bonding of 2-butyne in **1q-TSIns-yne** is very asymmetric, with one short (2.257 Å) and one long Ti.···C contact (2.537 Å). The latter carbon atom presents a contact of 2.365 Å with the methyl group. This contact is of the same order of magnitude as the N···C contact in **1q-TSCyc-yne** (2.397 Å). The insertion product **1q-Ins-yne** (Figure 3) is 86.8 kJ mol^{-1} more stable than **1q-π-yne** and features a weak γ-CH agostic interaction similar to that found for **4**.[14] The Ti···H_γ contact of 2.442 Å, together with the angles Ti−C_α−C_β (116.8°) and C_α−C_β−C_γ (119.9°) being smaller than the corresponding ones (Ti−C_α−Me = 118.6° and C_α−C_β−Me = 126.6°), speaks in favor of a weak γ-CH agostic interaction.

The results of the calculations on the simple model systems are schematically shown in Figure 4a. The $2\pi + 2\pi$ cycloaddition is kinetically and thermodynamically preferred over the insertion. To elucidate the origin of the kinetic preference for cycloaddition, a decomposition of the energy ($\Delta E^{\ddagger}$) of the TS **1q-TSIns-yne** and **1q-TSCyc-yne** was performed. The energy of the fragments $Ti(NMe)(H_3[9]aneN_3)Me^+$ and MeCCMe in the geometry they have in the two TS were evaluated in single-point B3PW91 calculations and were used, together with the energy of the TS, to estimate the interaction energy ΔE_{int}. These energies, together with the energy of the respective fragments in their optimal geometry, allow for the estimation of the deformation energies of the two fragments, ΔE_{def}(Ti) and ΔE_{def}(yne). As the energy of the TS, $\Delta E^{\ddagger}$, is evaluated with respect to the energy of the two separated fragments, the relation $\Delta E^{\ddagger} = \Delta E_{int} + \Delta E_{def}(Ti) + \Delta E_{def}(yne)$ holds. The values reported in Table 2 allow one to understand the origin of the kinetic preference.

In both cases (insertion and cycloaddition), the methyl cation has to distort to accommodate the incoming alkyne and the energetic cost of this process is independent of the alkyne orientation (axial in **1q-TSCyc-yne**, equatorial in **1q-TSIns-yne**). The methyl groups of the alkyne are less distorted in **1q-TSCyc-yne** than in **1q-TSIns-yne**, as illustrated by the values of the C≡C−Me angles (157.8 and 148.7°, **1q-TSCyc-yne**; 155.9 and 144.7°, **1q-TSIns-yne**), thus leading to a lower distortion energy ΔE_{def}(yne). The lower value of 144.7° in **1q-TSIns-yne** corresponds to the methyl group close to the equatorial NH group of the $H_3[9]aneN_3$ ligand. In both cases, the distortion energy of the alkyne is significantly larger than that of the cation, because greater rehybridization in the former is needed to increase the interaction with Ti.

The essential difference between the two reaction pathways comes from the nature of the leading interactions in the respective TS. The LUMOs of the distorted methyl cation are very similar in both **1q-TSCyc-yne** and **1q-TSIns-yne** and are typical σ-accepting orbitals developing in the vacant site. π back-donation from Ti to the alkyne would be expected to lead to a symmetric coordination. However, there is no occupied non-bonding orbital on the d^0 Ti to strengthen such a symmetric mode of coordination, and the alkyne has to adjust its orientation to seek back-donation from one of the highest occupied MOs of the cation. In **1q-TSIns-yne**, the back-donating MO is in fact the σ(Ti−Me) bond and this explains why the methyl group is tilted. Such a distortion leads to better overlap with the alkyne π^* orbital and is also associated with creation of an α-CH agostic interaction stabilizing the TS.[8b] The overall energetic cost of this tilting is apparently not very large (ΔE_{def}(Ti): **1q-TSIns-yne**, 37.2 kJ mol^{-1}; **1q-TSCyc-yne**, 34.6 kJ mol^{-1}).

In **1q-TSCyc-yne**, one π bond associated with π donation from the imido nitrogen is perfectly suited to achieve efficient back-donation. This is reflected by the significantly more negative value for ΔE_{int} (Table 2). The kinetic preference for cycloaddition appears thus to be essentially driven by the efficient back-donation of one Ti−N π bond into the alkyne π^* orbital. As this π bond is strongly developed on the more electronegative nitrogen atom, any modification of the steric bulk at the imido group could have a significant influence on the cycloaddition pathway.

In order to consider an increase of steric bulk at the cation only, a series of ONIOM(B3PW91:HF) calculations have been performed on the experimental monomethyl cation

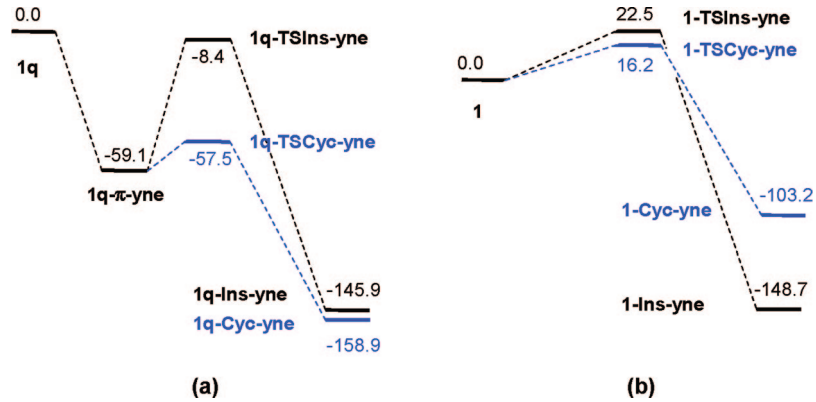

Figure 4. Schematic representation of the cycloaddition and insertion pathways for 2-butyne reacting with (a) **1q** or (b) **1**. B3PW91 energies (kJ mol^{-1}) are given. For the reactions with **1** the ONIOM(B3PW91:HF) optimized geometry was used in single-point B3PW91 calculations (B3PW91//ONIOM(B3PW91:HF)).

Table 2. Decomposition of the energy ($\Delta E^{\ddagger}$) of the TS for MeCCMe Cycloaddition (suffix TSCyc-yne) and Insertion (suffix TSIns-yne) with Respect to the Separated Reactants in Their Optimal Geometry as a Combination of an Interaction Term (ΔE_{int}) between the Fragments in the Geometry They Have in the TS, and the Deformation Energies (ΔE_{def}(Ti) and ΔE_{def}(yne)) Needed To Achieve These Geometries from the Optimal Ones[a]

	$\Delta E^{\ddagger}$	ΔE_{int}	ΔE_{def}(Ti)	ΔE_{def}(yne)
1q-TSIns-yne	−8.4	−124.8	37.2	79.2
1q-TSCyc-yne	−57.5	−158.1	34.6	66.0
1-TSIns-yne	22.5	−107.0	48.1	80.2
1-TSCyc-yne	16.2	−152.1	62.8	103.9

[a] The prefixes **1** and **1q** refer to calculations based on the cations Ti(N^{t}Bu)(Me$_3$[9]aneN$_3$)Me$^+$ (**1**) and Ti(NMe)(H$_3$[9]aneN$_3$)Me$^+$ (**1q**), respectively. Energies are given in kJ mol^{-1}.

Ti(N^{t}Bu)(Me$_3$[9]aneN$_3$)Me$^+$ (**1**) reacting with 2-butyne. In Figure 4b, the results of the ONIOM calculations are schematically represented to allow direct comparison with the calculations on the small model **1q**. No π-alkyne complex analogous to **1q-π-yne** could be optimized with the bulky cation **1**. The most striking features are (1) the cancelation of the kinetic preference for cycloaddition ($\Delta\Delta E^{\ddagger}$ = 6.3 kJ mol^{-1}, reaction of **1** vs 49.1 kJ mol^{-1}, reaction of **1q**) and (2) the strong thermodynamic preference for insertion (45.5 kJ mol^{-1}). The same energy decomposition used for **1q-TSCyc-yne** and **1q-TSIns-yne** was considered for **1-TSCyc-yne** and **1-TSIns-yne** using B3PW91 energies on the ONIOM(B3PW91:HF) geometries (B3PW91//ONIOM(B3PW91:HF)) for the various terms (see Table 2).

Interestingly, increasing the steric bulk does not lead to a substantial reduction of the interaction energy, ΔE_{int}. For **1-TSIns-yne**, the interaction is weaker by 17.8 kJ mol^{-1}, while in **1-TSCyc-yne**, the value differs by only 6.0 kJ mol^{-1} from that of **1q-TSCyc-yne**. The high energy of both TS ($\Delta E^{\ddagger}$ in Table 2) mainly originates from the distortions within each fragment. These distortions are necessary to achieve good interactions in the TS so that the activation barrier is not too high. For the insertion TS **1-TSIns-yne** the metal fragment undergoes an increase in the deformation energy of only 10.9 kJ mol^{-1} in comparison with **1q-TSIns-yne**; furthermore, the alkyne deformation is barely changed (1 kJ mol^{-1}). The main geometrical change in Ti(N^{t}Bu)(Me$_3$[9]aneN$_3$)Me$^+$ upon going from **1** to **1-TSIns-yne** is the elongation of the two equatorial Ti−N bonds to the Me$_3$[9]aneN$_3$ ligand by ca. 0.15 Å. In **1q-TSIns-yne**, the corresponding elongations are ca. 0.08 Å, showing the influence of introducing the Me group on the nitrogen atoms.

For **1-TSCyc-yne**, both partners experience much larger distortion when the steric bulk is introduced. For the metal fragment, the increase of 28.2 kJ mol^{-1} (ΔE_{def}(Ti), Table 2) is essentially due to a significant loss of Me$_3$[9]aneN$_3$ bonding to Ti in the TS. The three Ti−N bonds of the Me$_3$[9]aneN$_3$ ligand lengthen by ca. 0.2 Å from **1** to **1-TSCyc-yne**. In the small model system **1q-TSCyc-yne**, the equatorial Ti−N bonds do elongate, but by only 0.08 Å, and the apical Ti−N bond length remains the same. The elongation of the apical Ti−N bond in the real system **1-TSCyc-yne** is a direct consequence of steric repulsions developing between the alkyne and the N−Me group. Thus, in the TS for cycloaddition, the loss of bonding of the Me$_3$[9]aneN$_3$ ligand is larger than in the TS for insertion because the alkyne substituent interacts with the weakest Ti−N bond, the one trans to the strongly trans-labilizing imido ligand.[23] To accommodate the incoming alkyne, the imido could have bent away the ^{t}Bu group by decreasing the Ti═N−^{t}Bu angle, but this would have introduced a prohibitive energy cost due to loss of the strong Ti(3d$_\pi$)−N(2p$_\pi$) bonding interaction.[23] Indeed, the Ti═N−R angle is unchanged upon going from the small model cation **1q** (R = Me) to the cycloaddition TS **1q-TSCyc-yne** and decreases by only 5° on going from **1** to **1-TSCyc-yne** (R = ^{t}Bu).

The higher repulsions developing in the TS for cycloaddition are also visible in the alkyne fragment with an increase in distortion energy ΔE_{def}(yne) of 37.9 kJ mol^{-1} from **1q-TSCyc-yne** to **1-TSCyc-yne**. In the small model system **1q-TSCyc-yne**, the smallest C≡C−Me angle corresponds to the Me group oriented toward the H$_3$[9]aneN$_3$ ligand (148.7 vs 157.8°). In the real system **1-TSCyc-yne**, the relative order is unchanged but the values are significantly smaller (139.5 vs 151.0°), explaining the increase in distortion energy.

On the basis of the above results, there are clearly potential situations (i.e., bulky imides and/or alkynes) when insertion may become kinetically preferred over cycloaddition despite the electronic kinetic bias toward cycloaddition. We therefore turn finally to the full experimental system with PhCCPh (compound **4**, Scheme 1). The products of cycloaddition (**1-Cyc-ynePh**, hypothetical) and insertion (**1-Ins-ynePh** i.e., compound **4**) of PhCCPh with the real cation **1** have been optimized with ONIOM calculations (Figure S2 in the Supporting Information). The cycloaddition product is calculated to be 56.0 kJ mol^{-1} less stable than the insertion product, in agreement with **4** being the only observed isomer. This product energy difference is 10.5

(23) Kaltsoyannis, N.; Mountford, P. *J. Chem. Soc., Dalton Trans.* **1999**, 781.

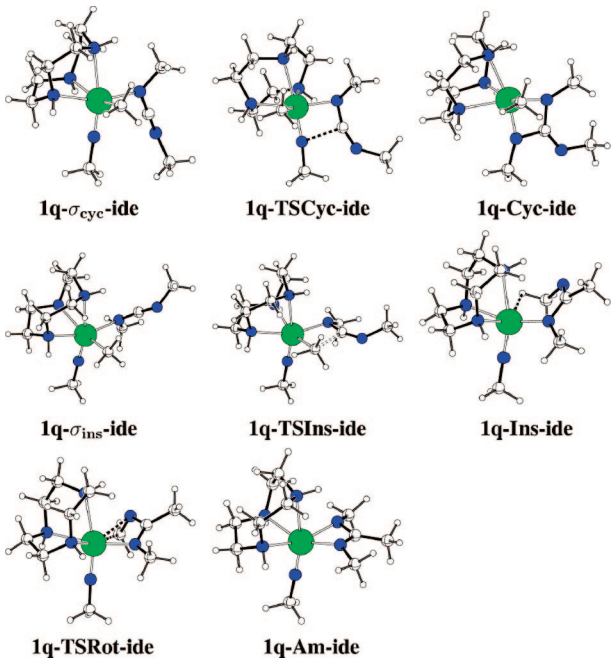

Figure 5. B3PW91 optimized geometries of the extrema located along the pathways for cycloaddition of MeNCNMe to Ti=NMe in $Ti(NMe)(H_3[9]aneN_3)Me^+$ (top) and insertion of MeNCNMe into Ti−Me (middle and bottom).

kJ mol^{-1} larger than that between **1-Ins-yne** and **1-Cyc-yne** (Figure 4) and is certainly a result of stronger repulsions between Ph and ^{t}Bu compared to those between Me and ^{t}Bu in **1-Cyc-yne**. These repulsions are best illustrated by the higher value for the energy (31.2 kJ mol^{-1}) of the TS, **1-TSCyc-ynePh**, for cycloaddition of PhCCPh to **1** (Figure S2) compared to the case for MeCCMe (16.2 kJ mol^{-1} for **1-TSCyc-yne**, Figure 4). For PhCCPh, the TS for insertion, **1-Ins-ynePh**, is even calculated to lie 5.8 kJ mol^{-1} lower in energy than **1-TSCyc-ynePh**. Thus, not only has the kinetic preference for cycloaddition been canceled but also in the present case insertion into Ti−Me has become the preferred pathway both kinetically and thermodynamically.

3. Reaction of Carbodiimides with Methyl and Chloride Titanium Imido Cations. Experimentally, the reaction of **1** with diisopropylcarbodiimide gave exclusively the Ti−Me migratory insertion product, namely the amidinate $Ti(N^tBu)(Me_3[9]aneN_3)\{MeC(N^iPr)_2\}^+$ (**5**; Scheme 1). Furthermore, even though $2\pi + 2\pi$ cycloaddition reactions between titanium imido complexes and carbodiimides (to form guanidinate complexes) are known,[5e] the reaction of the chloride cation **2** with ^{i}PrNCN^{i}Pr only yielded the σ adduct **8** (Scheme 1).

As an initial probe of these systems, the reaction of **1q**, as a model for **1**, with dimethylcarbodiimide was studied computationally so as to delineate the basic electronic features. The geometries of the extrema located along the pathways for cycloaddition and insertion are shown in Figure 5, and the energies, relative to the separated reactants, are reported in Table 3 and schematically represented in Figure 6.

For both pathways (cycloaddition and insertion) the first step is the formation of a very stable N-σ-adduct, **1q-σ_{cyc}-ide** and **1q-σ_{ins}-ide**, with the carbodiimide lying either parallel to the Ti=N bond vector or in the equatorial plane, respectively (Figure 5). The stability of these adducts is almost twice as large as that of the alkyne complex **1q-π-yne** (−59.1 kJ mol^{-1}, **1q-π-yne**; −114.8 kJ mol^{-1}, **1q-σ_{cyc}-ide**; −102.3 kJ mol^{-1}, **1q-σ_{ins}-ide**) as a result of the strong Lewis basicity of nitrogen lone pairs.

From **1q-σ_{cyc}-ide**, C−N coupling through **1q-TSCyc-ide** yields the cycloaddition guanidinate complex **1q-Cyc-ide** with a low activation barrier of 31.6 kJ mol^{-1} and an exothermic reaction energy of −47.8 kJ mol^{-1}. The cycloaddition of MeNCNMe from the σ adduct is less favored, both kinetically and thermodynamically, than cycloaddition of 2-butyne from the π complex, where the barrier was only 1.6 kJ mol^{-1} and the reaction was exothermic by nearly 100 kJ mol^{-1} (Figure 4). However, relative to the separated reactants, the thermodynamic stabilities of the cycloaddition products are similar (−158.9 kJ mol^{-1}, **1q-Cyc-yne**; −162.6 kJ mol^{-1}, **1q-Cyc-ide**).

Decomposition of the energy of the TS for cycloaddition of MeNCNMe, in a way similar to that described for the 2-butyne reactions in Table 2, yielded the following components: $\Delta E_{int} = -237.8$ kJ mol^{-1}; $\Delta E_{def}(Ti) = 36.0$ kJ mol^{-1}; ΔE_{def}(diimide) $= 118.6$ kJ mol^{-1}. The deformation of the methyl cation **1q** is very similar to that obtained for 2-butyne cycloaddition (34.6 kJ mol^{-1}, Table 2), but the deformation energy of the carbodiimide is significantly larger than the deformation energy of the alkyne (ΔE_{def}(yne) = 66.0 kJ mol^{-1}). However, the increased substrate destabilization is largely compensated for by the much stronger interaction (ΔE_{int}) between the methyl cation and MeNCNMe in the TS, compared to the case of 2-butyne ($\Delta E_{int} = -158.1$ kJmol^{-1}). This increased interaction energy mainly originates from the strong Ti−N adduct interaction already present in the σ adduct. The activation barrier of 31.6 kJ mol^{-1} from the σ adduct **1q-σ_{cyc}-ide** to **1q-TSCyc-ide** could be essentially ascribed to the energy cost associated with deformation of the carbodiimide.

From the alternative σ-adduct **1q-σ_{ins}-ide** (Figure 5), Me−C(=NMe)$_2$ coupling through **1q-TSIns-ide** yields the δ-Me agostic intermediate **1q-Ins-ide** (Figure 5). The activation barrier (from **1q-σ_{ins}-ide**) for MeNCNMe insertion into Ti−Me is 61.6 kJ mol^{-1}. This value, only slightly larger than that of the insertion of 2-butyne from **1q-π-yne** (50.7 kJ mol^{-1}, Figure 4), is nonetheless significantly higher than that for C−N coupling (cycloaddition) through **1q-TSCyc-ide** (31.6 kJ mol^{-1}). Decomposition of the energy of **1q-TSIns-ide** yielded the following contributions: $\Delta E_{int} = -185.3$ kJ mol^{-1}, $\Delta E_{def}(Ti) = 43.6$ kJ mol^{-1}, and ΔE_{def}(diimide) $= 101.1$ kJ mol^{-1}. As for the MeNCNMe cycloaddition reaction, the larger activation barrier (compared to the 2-butyne case) is essentially due to the larger energy cost for distorting the carbodiimide. However, a strong Ti−$N_{carbodiimide}$ interaction again stabilizes the entire energy profile. Perturbation of **1q-TSIns-ide** along the TS vector for insertion yielded the δ-Me agostic structure **1q-Ins-ide** in a very exothermic step ($\Delta E = -101.4$ kJ mol^{-1}). The Ti···Me_δ distance is 2.516 Å and two elongated agostic C−H bonds (C−H = 1.122 and 1.113 Å) are oriented toward Ti.

The first-formed product **1q-Ins-ide** thus contains a monodentate amidinate ligand with a relatively weak Ti···H−C interaction occupying a sixth coordination site at titanium. However, facile rotation around the β-CN bond of **1q-Ins-ide** ($\Delta E^{\ddagger} = 33.2$ kJ mol^{-1} via the TS **1q-TSRot-ide**) affords access to the very stable bidentate (κ^2(N,N)) amidinate complex **1q-Am-ide**, a model for the real complex **5** (Scheme 1). The energy of formation (ΔE) of **1q-Am-ide** is −320.7 kJ mol^{-1} with respect to **1q** + MeNCNMe. Therefore, in contrast to the case of 2-butyne (Figure 4a, $\Delta E = -145.9$ kJ mol^{-1}), there is an

Table 3. Energies (kJ mol^{-1}) of the Various Extrema for the Reaction between the Titanium Cations (1q, 2q, 1, 2) and Carbodiimides (MeNCNMe for Reaction with 1q and 2q; ^{i}PrNCN^{i}Pr for Reaction with 1 and 2)

	X-σ_{cyc}-ide	X-TSCyc-ide	X-Cyc-ide	X-σ_{ins}-ide	X-TSIns-ide	X-Ins-ide	X-TSRot-ide	X-Am-ide
X = 1q	−114.8	−83.2	−162.6	−102.3	−40.7	−203.7	−170.5	−320.7
X = 1	−69.3	−6.8	−71.6	−73.0	−5.9	−104.5	*a*	−245.2
X = 2q	−131.7	−85.6	−152.6	*a*	*a*	*a*	*a*	*a*
X = 2	−91.7	−5.8	−60.9	*a*	*a*	*a*	*a*	

[a] Not calculated.

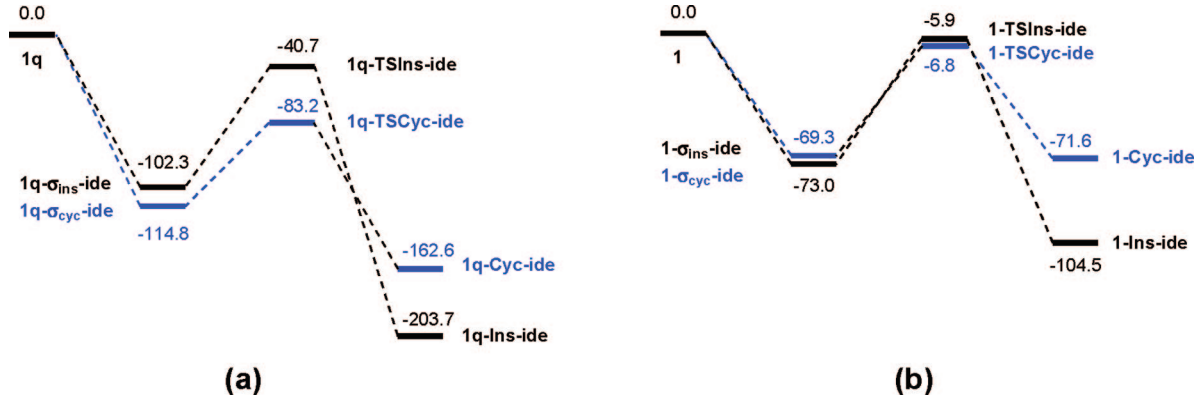

Figure 6. Schematic representation of the cycloaddition and insertion pathways for (a) **1q** reacting with MeNCNMe and (b) **1** reacting with ^{i}PrNCN^{i}Pr. B3PW91 energies (kJ mol^{-1}) are given. For the reactions with **1** the ONIOM(B3PW91:HF) optimized geometry was used in single-point B3PW91 calculations (B3PW91//ONIOM(B3PW91:HF)). For clarity the isomerization processes to the amidinate complexes (**1q-Am-ide** and **1-Am-ide**) are not shown.

extremely strong thermodynamic bias toward the insertion product for the reaction with MeNCNMe with **1q**.

Introduction of the actual experimental steric bulk by considering reaction of **1** with ^{i}PrNCN^{i}Pr at the ONIOM(B3PW91:HF) level showed interesting differences from those for the small model systems based on **1q** and MeNCNMe (Table 3). Due to the increased steric bulk, the formation energies of the σ adducts **1-σ_{cyc}-ide** and **1-σ_{ins}-ide** are reduced by 30−35 kJ mol^{-1} (Table 3), with the adduct lying in the equatorial plane (**1-σ_{ins}-ide**, the precursor to Ti−Me bond insertion) being marginally more stable than that aligned along the Ti=N bond vector (**1-σ_{cyc}-ide**). As for the results observed with **1** and 2-butyne (Figure 4b), introducing the experimental bulk resulted in a complete cancelation of the kinetic preference for cycloaddition ($\Delta\Delta E^{\ddagger}$ = 4.6 kJ mol^{-1}), since the TS for insertion (**1-TSIns-ide**) and cycloaddition (**1-TSCyc-ide**) are almost isoenergetic.

The products of cycloaddition and insertion are both significantly destabilized with respect to the results obtained on the small model system. Significantly, the cycloaddition product **1-Cyc-ide** is now isoenergetic with the σ adduct **1-σ_{cyc}-ide** and cycloaddition is expected to be a reversible, thermochemically neutral process. The energetics for the insertion pathway are different with the first-formed insertion product **1-Ins-ide** being ca. 30 kJ mol^{-1} more stable than the σ adduct (Table 3) and −104.5 kJ mol^{-1} more stable than the separated reactants. Like the smaller **1q-Ins-ide**, this κ^{1}(N)-bound intermediate features a δ-agostic C−H interaction between one of the amidinate ^{i}Pr groups and Ti (C−H = 1.135 Å, H···Ti = 2.182 Å). Subsequent rearrangement of **1-Ins-ide** forms the very stable bidentate amidinate complex **1-Am-ide**, which is stabilized by 140.7 kJ mol^{-1} relative to **1-Ins-ide** (−245.2 kJ mol^{-1} relative to separated **1** and ^{i}PrNCN^{i}Pr). No attempt was made to search for the TS linking **1-Ins-ide** and **1-Am-ide**, a facile process shown to be associated with rotation around the β-CN bond for the small system **1q-Ins-ide** ($\Delta E^{\ddagger}$ = 33.2 kJ mol^{-1}). The calculations on **1** and ^{i}PrNCN^{i}Pr account perfectly for the outcomes of the real systems (Scheme 1).

The results for **1** and ^{i}PrNCN^{i}Pr suggest that a σ adduct of the type **1-σ_{ins}-ide** or **1-σ_{cyc}-ide** should be thermodynamically stable, provided that the kinetically and thermodynamically favored Ti−Me insertion reaction could be blocked. Experimentally it was found that the chloride cation Ti(N^{t}Bu)(Me$_3$[9]aneN$_3$)Cl^{+} (**2**; Scheme 1), lacking a Ti−Me bond, formed a moderately stable adduct with ^{i}PrNCN^{i}Pr (**8**; Scheme 1). Reactions of MeNCNMe with Ti(NMe)(H$_3$[9]aneN$_3$)Cl^{+} (**2q**), a model for **2**, were therefore studied with B3PW91 calculations. The formation energy of the σ adduct **2q-σ_{cyc}-ide** is somewhat larger than for **1q** (−131.7 kJ mol^{-1} vs −114.8 kJ mol^{-1}, respectively; see Table 3). Substitution of Me in **1q** for Cl in **2q** renders the Ti cation more electrophilic and thus strengthens the N coordination. The stabilities of both the TS (**2q-TSCyc-ide**, −85.6 kJ mol^{-1}) and the product (**2q-Cyc-ide**, −152.6 kJ mol^{-1}) of cycloaddition are comparable to those obtained with **1q** (Table 3, −83 and −162.6 kJ mol^{-1}, respectively), and so the energetics associated with the cycloaddition reaction are indeed similar for **1q** and **2q**. However, because the initial σ adduct is more stable for **2q**, the overall result is a reduced thermodynamic preference, and higher activation barrier, for forming the cycloaddition product with **2q** compared to **1q**.

This effect is further illustrated by the ONIOM calculations on **2** (Table 3) reacting with ^{i}PrNCN^{i}Pr (modeling the real system **8**, Scheme 1). The formation energy of the σ adduct **2-σ_{cyc}-ide** is −91.7 kJ mol^{-1}, more favorable than for **1-σ_{cyc}-ide** (−69.3 kJ mol^{-1}). The TS for cycloaddition **2-TSCyc-ide** has virtually the same energy as that of **1-TSCyc-ide**, but because **2-σ_{cyc}-ide** is more stable than **1-σ_{cyc}-ide** it leads to a greater kinetic stability in the former case. Crucially, the cycloaddition product **2-Cyc-ide** is computed to be 30.8 kJ mol^{-1} less stable than **2-σ_{cyc}-ide**, removing any thermodynamic driving force for the reaction. Thus, both the energy of **2-σ_{cyc}-ide** and the relative energies of **2-σ_{cyc}-ide** and **2-Cyc-ide** are in perfect agreement with the experimental observations of an

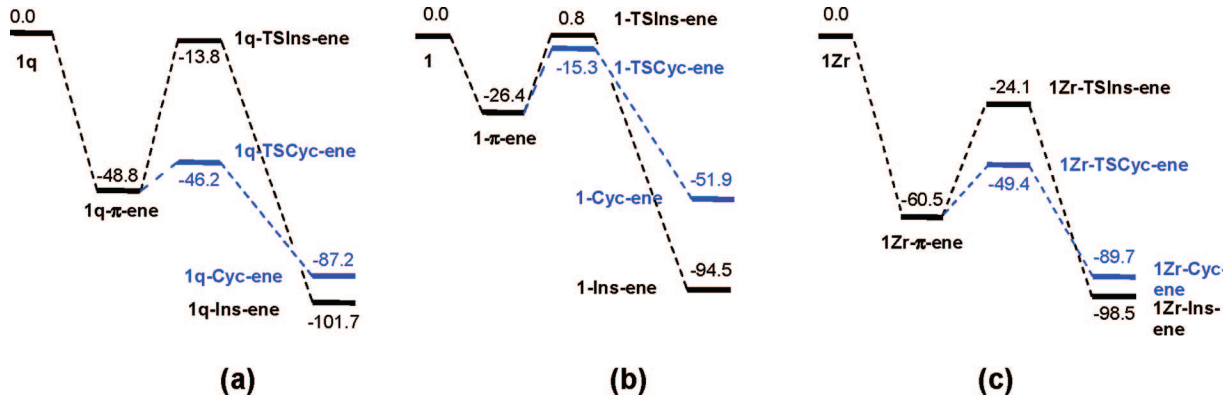

Figure 7. Schematic representation of the cycloaddition and insertion pathways for the reactions of C_2H_4 with (a) $Ti(NMe)(H_3[9]aneN_3)Me^+$ (**1q**), (b) $Ti(N^tBu)(Me_3[9]aneN_3)Me^+$ (**1**), and (c) $Zr(N^tBu)(Me_3[9]aneN_3)Me^+$ (**1Zr**). B3PW91 energies (kJ mol^{-1}) for the model system (**1q**) and ONIOM geometries (B3PW91//ONIOM(B3PW91:HF)) for the experimental system (**1**) have been used, respectively (kJ mol^{-1}).

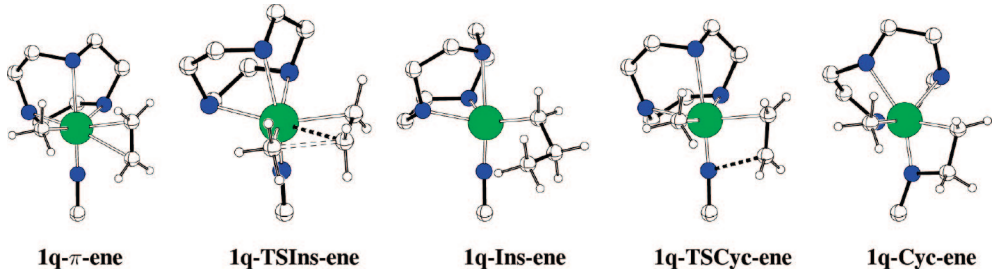

Figure 8. B3PW91 geometries of the extrema along the cycloaddition and insertion pathways for the reaction of **1q** with C_2H_4.

adduct between **2** and ^{i}PrNCN^{i}Pr and the lack of observation of any cycloaddition product.

4. Reactions of C_2H_4 with Group 4 Imido Cations: Titanium. The combined experimental[14] and theoretical studies of reactions of **1** with alkynes highlighted the critical role played by the nature of the imido substituent to obtain a given pathway among the various possible ones. A bulky group (e.g., ^{t}Bu) at the imido nitrogen significantly reduces the kinetic preference for cycloaddition to the Ti=NR bond with respect to insertion into the Ti−alkyl bond. The effect is even more pronounced with respect to thermodynamic selectivity, with insertion being observed when bulky groups are present on the nitrogen. The above results agree nicely with the experimental observations in structure/activity relationships observed in polymerization studies with MAO-activated $Ti(NR)(Me_3[9]aneN_3)Cl_2$ catalysts.[12]

Of particular relevance to our work are recent DFT calculations by Jensen and Børve on aspects of Gibson's bis(imido)chromium catalysts $Cr(NR)_2R'_2$.[11] It was found that C_2H_4 addition to the Cr=NR bond in $Cr(NR)_2Me^+$ was facile, although surprisingly the reaction and activation energies changed little (or not at all) between R = Me and R = ^{t}Bu. However, they were not able to clarify the consequences of these findings with regard to catalyst activity, nor were any comparisons made between Cr−Me insertion and Cr=NR cycloaddition reactions for chemically realistic systems (i.e., for Cr=NR other than Cr=NH). To clarify these issues and to gain some insight into the real catalyst systems $Ti(NR)(Me_3[9]aneN_3)Cl_2$, the reactions of **1q** and **1** with ethylene were studied computationally. Figure 7 shows the relative energies of the various species, Figure 8 illustrates some structures, and Table 4 gives key energies of the extrema.

As a starting point, reactions of the small model system **1q** with C_2H_4 were calculated at the DFT level. The results for the insertion and cycloaddition pathways are shown in Figure 7a. As in the case of the reaction with 2-butyne (Figure 4a), only a π adduct (**1q-π-ene**) with the C=C bond along the Ti=N vector could be optimized with a stabilization energy of −48.8 kJ mol^{-1} (Figure 8). The ethylene (**1q-π-ene**) and 2-butyne (**1q-π-yne**, Figure 4a) complexes have similar stabilities, as previously observed by Straub and Bergman.[4] The cycloaddition activation barrier (2.6 kJ mol^{-1} via TS **1q-TSCyc-ene**) to form the azacyclobutane species **1q-Cyc-ene** is very low and similar to that obtained for 2-butyne cycloaddition. However, the formation of the azacyclobutane **1q-Cyc-ene**, while reasonably exothermic (−87.2 kJ mol^{-1}), is much less thermodynamically favored than formation of the azacyclobutene **1q-Cyc-yne** (−158.9 kJ mol^{-1}, Figure 4a) in the case of 2-butyne. Indeed, Bergman and Andersen found that the reaction of C_2H_4 with $Cp^*_2Ti(NPh)$ is reversible.[16] In the reaction of C_2H_4 with $Ti(NPh)(^tBuSiO)_2$, Bennet and Wolczanski found that there was cycloaddition which appeared not to lose C_2H_4 during a fluxional process but did appear to show a dynamic equilibrium between the cycloaddition product and a π-complex.[17]

Table 4. Energies (kJ mol^{-1}) of the Reactants, TS, and Products Associated with Reactions of C_2H_4 with Various Ti Cations[a]

	cycloaddition			insertion		
	π adduct	TS	product	π adduct	TS	product
1q + C_2H_4	−48.8	−46.2	−87.2	−48.8	−13.8	−101.7
1 + C_2H_4	−26.4	−15.3	−51.9	−26.4	0.8	−94.5
1q-Ins-ene + C_2H_4	−44.4	−42.1	−84.0	−44.4	−23.1	−115.0
1-Ins-ene + C_2H_4	*b*	−6.5	−44.2	*b*	−6.4	−114.9
1q-Cyc-ene + C_2H_4	*c*	*c*	*c*	*b*	108.2	−88.1
1-Cyc-ene + C_2H_4	*c*	*c*	*c*	*b*	183.8	−76.0

[a] Energies are given relative to separated C_2H_4 and considered cation. [b] No π adduct could be located on the PES. [c] Cycloaddition to **1q-Cyc-ene** is not possible.

As observed with 2-butyne, ethylene insertion into Ti−Me is more costly in terms of activation energy ($\Delta E^{\ddagger} = 35$ kJ mol^{-1} via the TS **1q-TSIns-ene**) and so is kinetically disfavored. However, in contrast to the reaction with 2-butyne, the insertion product **1q-Ins-ene** (−101.7 kJ mol^{-1}) is more stable than the cycloaddition product by ca. 14.5 kJ mol^{-1} (for 2-butyne **1q-Cyc-yne** is more stable than **1q-Ins-yne** by 13 kJ mol^{-1}). To make a better comparison between the insertion/cycloaddition reactions of **1q** and alkenes and alkynes, we also calculated the reaction of **1q** with HCCH. In this case the insertion (relative to cycloaddition) is kinetically disfavored by 32.7 kJ mol^{-1} and slightly thermodynamically favored by 2.7 kJ mol^{-1}. It appears that in terms of *relative* Ti−Me/Ti═NMe reactivities, reaction at the Ti−Me bond is intrinsically thermodynamically favored. However, Figures 4a and 7a show that the intrinsic behavior of **1q** toward 2-butyne or C_2H_4 is the same: cycloaddition is strongly preferred over insertion kinetically.

ONIOM(B3PW91:HF) calculations on reaction of the real system **1** with C_2H_4 were also carried out, and the results are shown schematically in Figure 7b. The results are similar to those obtained with 2-butyne, except that a π adduct (**1-π-ene**) could be optimized. However, the kinetic preference for cycloaddition is significantly reduced, as judged by differences between the respective TSs ($\Delta\Delta E^{\ddagger} = 16.1$ for **1** + C_2H_4 vs 32.4 kJ mol^{-1} for **1q** + C_2H_4) and, more importantly, the thermodynamic preference for insertion is strongly reinforced (42.5 kJ mol^{-1} in favor of **1-Ins-ene** vs 14.5 kJ mol^{-1} in favor of **1q-Ins-ene**).[24]

Therefore, as in the case of the reaction with internal alkynes (Figure 4), inclusion of a bulky group at the imido nitrogen leads to a significant *decrease* in the kinetic bias toward cycloaddition and a thermodynamic *decrease* in stability of the Ti═NR cycloaddition product. In the case of C_2H_4 this latter effect becomes more important, since the energy of formation of cycloaddition products is already much less than for the alkynes, as is already apparent for the small model **1q**. As Figure 7b shows for **1** + C_2H_4, the energy of **1-Cyc-ene** is in fact only −51.9 kJ mol^{-1} relative to the separated reactants and so is at the limit of thermodynamic stability (in terms of Gibbs free energy) once entropic effects are taken into account. In this regard we recall that experimentally the chloride cation **2** (Scheme 1) did not react with C_2H_4 or other alkenes. Calculations on **2** at the ONIOM level showed that formation of a cycloaddition product was favorable but had an energy of −47.4 kJ mol^{-1}, consistent with the experimental observations and the results for **1** + C_2H_4 described above.

As increasing the length of the alkyl chain introduces steric bulk in the equatorial plane, it was thus of interest to study how ethylene insertion into the Ti−CH_2CH_2Me bond of **1q-Ins-ene** relates to cycloaddition to Ti═NMe in the same product. A π adduct of C_2H_4 with **1q-Ins-ene**, similar to **1q-π-ene**, was located and the formation energy of −44.4 kJ mol^{-1} is very similar to that for **1q-π-ene** (−48.8 kJ mol^{-1}, Table 4). The activation barrier for cycloaddition is virtually unchanged (2.6 kJ mol^{-1} for **1q** vs 2.3 kJ mol^{-1} for **1q-Ins-ene**) and cycloaddition remains the kinetically preferred pathway for C_2H_4 reacting with **1q-Ins-ene**. Introducing a bulkier alkyl chain at Ti therefore does not alter dramatically the relative kinetic preferences regarding insertion vs cycloaddition.

However, as expected, the activation barrier for the second insertion is lower than for the first one (35.0 kJ mol^{-1} for **1q** vs 21.3 kJ mol^{-1} for **1q-Ins-ene**, Table 4). In fact, the geometry of the α-CH agostic interaction developing in the TS for insertion speaks in favor of a more stable situation for the second insertion (Ti−C = 2.155 Å, C−H = 1.121 Å, Ti−C−H = 73°, first insertion; Ti−C = 2.137 Å, C−H = 1.130 Å, Ti−C−H = 70°, second insertion). The second insertion is also thermodynamically more favorable (−52.9 kJ mol^{-1}, first insertion; −70.6 kJ mol^{-1}, second insertion). The consequence is an increased energy difference between the two potential products of reaction of C_2H_4 with **1q-Ins-ene**. The insertion product is 31 kJ mol^{-1} more stable than the cycloaddition product, whereas in the reaction of **1q** with ethylene, the insertion product, **1q-Ins-ene**, was only 14.5 kJ mol^{-1} more stable than the cycloaddition product, **1q-Cyc-ene**. Thus, from an electronic point of view, reaction of C_2H_4 with the insertion product **1q-Ins-ene** is still kinetically likely to undergo cycloaddition to Ti═NMe but the kinetic preference for cycloaddition has been reduced, and the thermodynamic preference for insertion is increased.

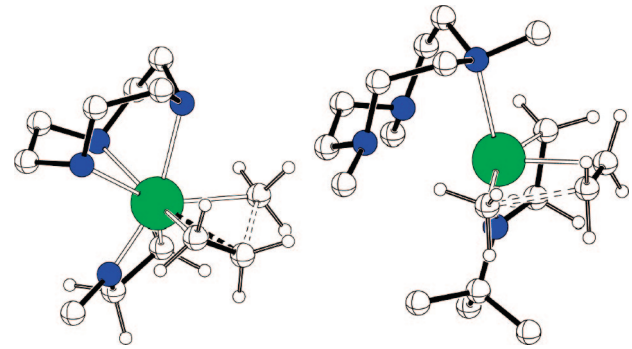

Figure 9. Optimized geometry (B3PW91, left; ONIOM(B3PW91:HF), right) of the TS for insertion of a second ethylene into the Ti−Me bond of **1q-Cyc-ene** (left) and **1-Cyc-ene** (right). Only the H atoms on the Ti−Me and C_2H_4 are shown.

The energy difference ($\Delta\Delta E^{\ddagger}$) between the two TSs for cycloaddition and insertion of C_2H_4 with **1-Ins-ene** is only 0.1 kJ mol^{-1} (Table 4), whereas it was 16.1 kJ mol^{-1} in favor of cycloaddition for the first reacting ethylene. Increasing the bulk at the imido ligand and extending the alkyl chain has therefore completely canceled the kinetic preference for cycloaddition. Moreover, the energy difference between the two products is also significantly increased with the product of the second insertion for **1-Ins-ene** now 70.7 kJ mol^{-1} more stable than the product of cycloaddition (cf. 42.6 kJ mol^{-1} in favor of the insertion product for the reaction of the first C_2H_4; Table 4).

In the case of nonbulky imido groups the cycloaddition pathway is kinetically preferred and it was therefore important to test if polymerization reactivity (i.e., Ti−Me insertion) is still possible on a cycloaddition product (**1q-Cyc-ene** or **1-Cyc-ene**). To this end, the TS for C_2H_4 insertion into Ti−Me in **1q-Cyc-ene** has been located and its geometry is shown in Figure 9. No precomplex could be located on the PES, and the activation barrier for C_2H_4 insertion into Ti−Me for **1q-Cyc-ene** amounts to 108.2 kJ mol^{-1} (Table 4). The high activation barrier is the result of a very distorted geometry around a seven-coordinate Ti center. The methyl group migrating to the incoming C_2H_4 is best described as a capping ligand with a long Ti−C bond (2.327 Å) and a rather weak α-CH agostic interaction (C−H = 1.102 Å, Ti−C−H = 80.2°). The geometrical parameters are in contrast with those for the other insertion TS, where the Ti−C bond distance was ca. 2.15 Å.

The geometry of the TS for C_2H_4 insertion into the Ti−Me bond of the cycloaddition product **1-Cyc-ene**, which contains

(24) For the insertion reaction of **1q** or **1** with C_2H_4, a β-agostic complex was found to be slightly more stable than **1q-Ins-ene** or **1-Ins-ene** (−10.8 and −17.2 kJ mol^{-1}, respectively).

the experimental ligands, is also shown in Figure 9. The activation barrier for C_2H_4 insertion into Ti−Me of the cycloaddition product **1-Cyc-ene** amounts to 183.8 kJ mol^{-1} (Table 4). In this case, however, the high energy of the TS is not the result of a seven-coordinate geometry around Ti as observed for the model systems. In fact, the migrating methyl group is only 2.166 Å from Ti and the α-CH agostic interaction is typical for these systems (C−H = 1.115 Å, Ti−C−H = 78.7°). The main reason for the high energy of this TS is the partial decoordination of the Me_3[9]aneN$_3$ ligand with the two equatorial Ti···N distances significantly longer than in **1-Cyc-ene** (2.581 and 3.621 Å). The decoordination of the Me_3[9]aneN$_3$ ligand is a response of the system to the steric pressure in the TS and corresponds to dissociation of the more weakly bonded ligand. This process is extremely costly energetically, and the TS for Ti−Me insertion on the cycloaddition product **1-Cyc-ene** lies at very high energy.

5. Reactions of C_2H_4 with Group 4 Imido Cations: Zirconium. Many efficient olefin polymerization catalysts are based upon Zr.[7] We were therefore interested in investigating how the substitution of Ti for Zr in the catalyst system **1** would alter the selectivity for cycloaddition or insertion, since the influence of the steric bulk at the imido ligand is expected to vary with the bigger Zr metal. Experimentally, catalytic studies of Zr systems such as Zr(N^{t}Bu)(Me_3[9]aneN$_3$)X$_2$ (X = Cl, Me) and Zr(N^{t}Bu)(Me_3[9]aneN$_3$)Me$^+$ have yet to be reported, and so DFT studies of these systems will help guide further studies in this area.

ONIOM(B3PW91:HF) calculations have been carried out on the complex Zr(N^{t}Bu)(Me_3[9]aneN$_3$)Me$^+$ (**1Zr**) reacting with C_2H_4. Only the competition between Zr−Me insertion and Zr=N^{t}Bu cycloaddition of the first ethylene molecule has been studied. In the case of Zr, two different π adducts, **1Zr-π_N-ene** and **1Zr-π_C-ene**, were obtained, depending on the position of the coordinated ethylene molecule (aligned with Zr=N or in the equatorial plane, respectively). As in the case of Ti, the preferred interaction is along the Zr=N bond with a formation energy of −60.5 kJ mol^{-1} for **1Zr-π_N-ene**, while the formation energy of **1Zr-π_C-ene** is −40.5 kJ mol^{-1}. Activation barriers are evaluated from the more stable complex **1Zr-π_N-ene**. Formation of these π adducts is significantly more favored thermodynamically in comparison to the titanium system, where the complex **1-π** was only 26.4 kJ mol^{-1} more stable than the separated reactants. This is consistent with expected metal−ligand bonding energy trends going down a transition-metal triad.

Figure 7c shows schematically the energetics of the two pathways. Interestingly, the activation barrier for cycloaddition to Zr=N^{t}Bu from **1Zr-π_N-ene** is identical with that obtained for cycloaddition from the Ti analogue **1-π-ene** (11.1 kJ mol^{-1}), and the product of cycloaddition, **1Zr-Cyc-ene**, is 29.2 kJ mol^{-1} more stable than **1-π_N-ene** (the reaction was exothermic by 25.5 kJ mol^{-1} for Ti). For the cycloaddition reaction, the kinetic and thermodynamic parameters for Zr are very similar to those obtained for Ti. The only difference is the greater stability of the π adduct, with the consequence that the entire energy profile is pulled down in energy. This sets the cycloaddition product at an energy (relative to separated reactants) comparable to **1q-Cyc-ene**, the cycloaddition product on the small model system for Ti (**1q**).

The activation barrier for insertion is 36.4 kJ mol^{-1} (cf. 27.2 kJ mol^{-1} for Ti (**1**)), and the insertion product, **1Zr-Ins-ene**, is 38.0 kJ mol^{-1} more stable than the π adduct **1Zr-π_N-ene**. However, **1Zr-Ins-ene** is only 8.8 kJ mol^{-1} more stable than **1Zr-Cyc-ene** (Figure 7c). In the case of Ti, this difference was larger (42.6 kJ mol^{-1} between **1-Cyc-ene** and **1-Ins-ene**, Figure 7b), introducing a strong thermodynamic bias toward insertion. With Zr, this thermodynamic preference is much reduced, essentially because the cycloaddition product is less destabilized, as judged from the relative energies with respect to separated reactants (−89.7 kJ mol^{-1}, **1Zr-Cyc-ene**; −98.5 kJ mol^{-1}, **1Zr-Ins-ene**; −51.9 kJ mol^{-1}, **1-Cyc-ene**; −94.5 kJ mol^{-1}, **1-Ins-ene**). Therefore, although the insertion products for Ti and Zr have similar stabilities with respect to the respective methyl cations and ethylene, the deciding factor in these competitive site-selectivity reactions is stronger competition from the alternative Zr=NR + C_2H_4 cycloaddition process.

Despite the thermodynamic near-equivalence of **1Zr-Cyc-ene** and **1Zr-Ins-ene**, kinetically the cycloaddition pathway remains significantly preferred over that of insertion (Figure 7c). The energy difference between the two TS is 25.3 kJ mol^{-1} in favor of the cycloaddition, while it was 16.1 kJ mol^{-1} in the case of Ti. Again, this is a result of the strong interaction developing between Zr and C_2H_4 in the π adduct. Thus, the above calculations indicate that the cycloaddition pathway is likely to remain the preferred pathway, both kinetically and thermodynamically, in the case of the Zr cation **1Zr**. Even a bulky *tert*-butyl group on the imido nitrogen is not enough to block the cycloaddition, and therefore the Zr analogue of **1**, if made, is expected to yield poor catalytic activity in olefin polymerization.

Conclusions

Our comprehensive DFT and ONIOM calculations firmly show that cycloaddition is electronically the preferred pathway as interaction between the imido π bond and the π^* orbital on the organic substrate lowers the energy of the transition state. However, the imido ligand—being strongly bonded to Ti—cannot easily be distorted. In contrast, the neutral Me_3[9]aneN$_3$ ligand is less strongly bonded and is thus able to experience larger distortion at a (comparatively) lower energy cost. Any reaction pathway that involves a strong interaction with the imido ligand (i.e., cycloaddition) is strongly influenced by the steric bulk at the imido nitrogen.

For the terminal alkyne PhCCH, the preferred cycloaddition pathway is followed providing the substrate interacts with the Ti methyl cation without introducing steric repulsions. This leads to the observation of only one regioisomer with the nonbulky group (H) close to ^{t}Bu. For the internal alkynes, even with the small 2-butyne, the kinetic preference for cycloaddition is almost canceled and the thermodynamic preference for insertion is magnified.

For the reactions with carbodiimides, an essential feature is the strong stabilization associated with N coordination. This is illustrated by the observation of the insertion product in the reaction of **1** with ^{i}PrNCN^{i}Pr, because a κ^2N amidinate complex is obtained. In the case of the more electrophilic Ti center in **2**, the σ adduct is strongly stabilized with respect to the cycloaddition product and, as no insertion is possible, only N coordination of the carbodiimide is observed.

For the reactions with ethylene, even though the substrate is small, the kinetic preference for cycloaddition is lowered when the bulk at the imido ligand is considered. The ONIOM calculations clearly show that, for a propagating alkyl chain, steric bulk at the imido ligand will selectively orient the incoming ethylene molecule toward the insertion pathway by blocking access to the electronically preferred cycloaddition pathway. This selectivity is enhanced once the bulk of the alkyl chain is increased, and even for the first step studied here,

namely Ti−Me → Ti−Pr, the gain in selectivity is dramatic. These calculations with C_2H_4 clearly show that when the catalyst is subject to a cycloaddition reaction it loses its catalytic properties toward polymerization and becomes inactive. Therefore, it is crucial to protect the system against such cycloaddition reactions, and the calculations have shown that increased steric bulk at the imido ligand is a very efficient means to achieve this goal without adversely affecting the kinetic or thermodynamic aspects of the Ti−R insertion reactions.

However, changing the metal is noninnocent, as the calculations on the Zr system show that the "blocking" effect of the bulk at imido for cycloaddition is less efficient with regard to selectively tuning the system toward insertion reactivity. Therefore, from the calculations it is predicted that the Zr analogue of **1** is likely to present a lower catalytic activity even with large groups at the imido ligand.

Computational Details

All the calculations have been performed with the Gaussian03 package.[25] For the DFT calculations, the functional chosen was the hybrid functional B3PW91.[26] For the experimental systems, ONIOM(B3PW91:HF) calculations[27] were performed, where the methyl groups on the Me_3[9]ane$_3$ ligand, the ^{t}Bu group of imido, and the ^{i}Pr group of carbodiimide, together with the Ph groups on PhCCH and PhCCPh, were treated at the HF level. For the DFT calculations (including the higher level part of the ONIOM calculations) the titanium and zirconium atoms were represented by the relativistic effective core potential (RECP) from the Stuttgart group (12 valence electrons) and the associated basis set,[28] augmented by an f polarization function.[29] The Cl atom was represented by RECP from the Stuttgart group and the associated basis set,[30] augmented by a d polarization.[31] The remaining atoms (C, H, N) were represented by a 6-31G(d,p) basis set.[32] For the lower level in the ONIOM calculations treated at the HF level, the Ti, Zr, and Cl atoms were treated with the Los Alamos RECP and the associated basis set,[33] while the remaining atoms were treated with a 4-31G basis set. Full optimizations of geometry without any constraint were performed, followed by analytical computation of the Hessian matrix to confirm the nature of the located extrema as minima or transition states on the potential energy surface. The estimated geometries for the TS were constructed on the basis of typical geometrical data for cycloaddition and insertion transition states already studied by us. The natures of the reactant and product connected through a given TS were confirmed by optimization to minima of slightly altered geometries of the TS in both directions along the transition state vector. NMR chemical shifts were computed using the GIAO method[34] at the B3PW91 level. For the NMR parameters, all-electron calculations were considered where the basis set for Ti was the TZP basis set of Ahlrichs,[35] and all the other atoms were described with the IGLO-II basis set.[36]

Acknowledgment. We thank the EPSRC (P.D.B.), CNRS (E.C.), Egide and the British Council (E.C. and P.M.), and the MESR and the Spanish Ministerio de Educación y Ciencia (M.F.) for support.

Supporting Information Available: Geometries of the three σ-CH complexes of PhCCH with **1** (Figure S1), geometries of the TSs and products for the cycloaddition and insertion reactions of PhCCPh with **1** (Figure S2), a comparison of the energies of the TS for PhCCH reacting with **1** with different DFT functionals (Table S1), a comparison of the B3PW91 and ONIOM(B3PW91:HF) geometries for the TS of the reaction of PhCCH with **1** (Table S2), text giving the complete reference for Gaussian 03, and tables giving Cartesian coordinates for the molecules optimized and their electronic energies (B3PW91 single-point energy on the ONIOM geometry for the ONIOM calculations). This material is available free of charge via the Internet at http://pubs.acs.org.

OM8007103

(25) Pople, J. A.,et al. Gaussian 03, revision C02; Gaussian Inc., Wallingford, CT, 2004.
(26) (a) Becke, A. D. *J. Chem. Phys.* **1993**, *98*, 5648. (b) Perdew, J. P.; Wang, Y. *Phys. Rev. B* **1992**, *45*, 13244.
(27) Svensson, M.; Humbel, S.; Froese, R. D. J.; Matsubara, T.; Sieber, S.; Morokuma, K. J. *J. Phys. Chem.* **1996**, *100*, 19357.
(28) For Ti: Dolg, M.; Wedig, U.; Stoll, H.; Preuss, H. *J. Chem. Phys.* **1987**, *86*, 866. For Zr: Andrae, D.; Haussermann, U.; Dolg, M.; Stoll, H.; Preuss, H. *Theor. Chim. Acta* **1990**, *77*, 123.
(29) Ehlers, A. W.; Bohme, M.; Dapprich, S.; Gobbi, A.; Hollwarth, A.; Jonas, V.; Kohler, K. F.; Stegmann, R.; Veldkamp, A.; Frenking, G. *Chem. Phys. Lett.* **1993**, *208*, 111.
(30) Bergner, A.; Dolg, M.; Kuchle, W.; Stoll, H.; Preuss, H. *Mol. Phys.* **1993**, *80*, 1431.
(31) Hollwarth, A.; Bohme, M.; Dapprich, S.; Ehlers, A. W.; Gobbi, A.; Jonas, V.; Kohler, K. F.; Stegmann, R.; Veldkamp, A.; Frenking, G. *Chem. Phys. Lett.* **1993**, *208*, 237.
(32) Hariharan, P. C.; Pople, J. A. *Theor. Chim. Acta* **1973**, *28*, 213.
(33) (a) Wadt, W. R.; Hay, P. J. *J. Chem. Phys.* **1985**, *82*, 284. (b) Wadt, W. R.; Hay, P. J. *J. Chem. Phys.* **1985**, *82*, 299.
(34) (a) Lee, A. M.; Handy, N. C.; Colwell, S. M. *J. Chem. Phys.* **1995**, *103*, 10095. (b) Ditchfiled, R. J. *Chem. Phys. Lett.* **1972**, *56*, 5688.
(35) Schäfer, A.; Huber, C.; Ahlrichs, R. J. *Chem. Phys. Lett.* **1994**, *100*, 5829.
(36) Kutzelnigg, W.; Fleischer, U.; Schindler, M. *The IGLO-Method: Ab Initio Calculation and Interpretation of NMR Chemical Shifts and Magnetic Susceptibilities*; Springer-Verlag: Heidelberg, Germany, 1990; Vol. 23.